

# IS-DARTS: Stabilizing DARTS through Precise Measurement on Candidate Importance

Hongyi He, Longjun Liu\*, Haonan Zhang, Nanning Zheng

National Key Laboratory of Human-Machine Hybrid Augmented Intelligence, National Engineering Research Center for Visual Information and Applications, and Institute of Artificial Intelligence and Robotics, Xi'an Jiaotong University  
hongyihe@stu.xjtu.edu.cn, liulongjun@xjtu.edu.cn, haonanzhang@stu.xjtu.edu.cn, nnzheng@xjtu.edu.cn

## Abstract

Among existing Neural Architecture Search methods, DARTS is known for its efficiency and simplicity. This approach applies continuous relaxation of network representation to construct a weight-sharing supernet and enables the identification of excellent subnets in just a few GPU days. However, performance collapse in DARTS results in deteriorating architectures filled with parameter-free operations and remains a great challenge to the robustness. To resolve this problem, we reveal that the fundamental reason is the biased estimation of the candidate importance in the search space through theoretical and experimental analysis, and more precisely select operations via information-based measurements. Furthermore, we demonstrate that the excessive concern over the supernet and inefficient utilization of data in bi-level optimization also account for suboptimal results. We adopt a more realistic objective focusing on the performance of subnets and simplify it with the help of the information-based measurements. Finally, we explain theoretically why progressively shrinking the width of the supernet is necessary and reduce the approximation error of optimal weights in DARTS. Our proposed method, named IS-DARTS, comprehensively improves DARTS and resolves the aforementioned problems. Extensive experiments on NAS-Bench-201 and DARTS-based search space demonstrate the effectiveness of IS-DARTS.

## 1 Introduction

Although neural networks have achieved significant success in numerous computer vision domains(He et al. 2016; Ren et al. 2015; Long, Shelhamer, and Darrell 2015), designing neural architectures remains an uphill task demanding extensive expertise and repeated fine-tuning. In recent years, researchers have endeavored to discover Neural Architecture Search (NAS) methods that automate the manual process of exploiting outstanding architectures. Previous NAS methods based on reinforcement learning(Baker et al. 2016; Zoph et al. 2018; Pham et al. 2018) and evolutionary algorithm(Real et al. 2017; Liu et al. 2017; Real et al. 2019) typically require thousands of GPU days computational resources, which impede their practical application. Therefore, one-shot methods(Liu, Simonyan, and Yang

2018; Chen et al. 2019; Chu et al. 2020b,a) are proposed, which complete searching in one training of the supernet containing all potential subnets with weight sharing strategy.

Among many proposed approaches, Differential ARchitecture Search (DARTS)(Liu, Simonyan, and Yang 2018) leverages architecture parameters to continuously relax the discrete search space, enabling gradient backpropagation in the supernet. DARTS enhances the search efficiency by a large margin while achieving comparable performance. However, some studies(Chen et al. 2019; Zela et al. 2019; Chu et al. 2020b) report that DARTS suffers from performance collapse due to the dominance of parameter-free operations in the selected architecture. Existing solutions to this problem vary considerably, including imposing hand-crafted rules(Chu et al. 2020b,a), suppressing the indicator(Liang et al. 2019; Zela et al. 2019) and so on. However, the vast majority rely on the prior knowledge that performance collapse will happen, which cure the symptoms instead of the disease. Moreover, many methods lack theoretical analysis on their relationship with the original optimization problem, making them less persuasive.

This paper is dedicated to analyzing and resolving the problems leading DARTS to suboptimal results, including but not limited to the above two problems. We prove theoretically and experimentally that the architecture parameters in the supernet fail to represent the importance of the candidate operations in the search space. As a result, the subnet selected by the magnitude of architecture parameters undisputedly performs disastrously. In response, we measure the importance more precisely through the information in the intermediate feature maps output by the operations. We also prove that nodes in a subnet retaining more important operations output more informative and significant feature maps.

Furthermore, we find that the losses minimized in in the bi-level optimization objective of DARTS are all concerned with the supernet. We reformulate the objective with binary masks and turn its attention to the performance of the subnets, which should be the primary objective of DARTS. In addition, the training set encounter a forcible split for the training of the network weights and the architecture parameters, which reduces the efficiency of data utilization. We emancipate the validation set in the objective function and calculate more precise weights with the help of the importance measurement.

\*Longjun Liu is the corresponding author.

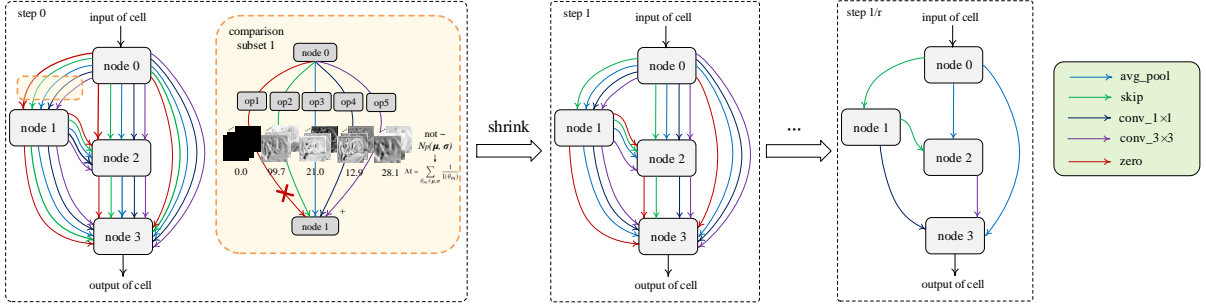


Figure 1: Overall illustration of IS-DARTS. The searching process of only one cell in the supernet is displayed for simplicity. The operations in one comparison subset(one edge for example in the figure) are compared and gradually discarded through the information-based metric.

Last, the approximation in the objective introduces error into the training of the network weights, which in turn affects the identification of good subnets. We explain the necessity for introducing multi-step shrinking in order to decrease the approximation errors. Following previous researches(Chen et al. 2019; Li et al. 2020; Wang et al. 2021b), we explore to progressively shrink the operations in a defined comparison subset, which connects the supernet with the subnet step by step.

The proposed method, named Information-based Shrinking DARTS (IS-DARTS), is illustrated in Figure 1. Extensive experiments on various search spaces and datasets manifest the great potential of the proposed IS-DARTS, which achieve better performance while costing less computational resources. On NAS-Bench-201, we achieve the same state-of-the-art results in 4 independent runs with only 2.0 GPU hours. The implementation of IS-DARTS is available at <https://github.com/HY-HE/IS-DARTS>.

## 2 Related Works

The efforts made to address the performance collapse of DARTS(Liu, Simonyan, and Yang 2018) can be roughly divided into two parts.

The first type is based on the searching supernet. Fair DARTS(Chu et al. 2020b) utilizes sigmoid functions instead of softmax to convert the exclusive competition into a cooperative relationship. DARTS-(Chu et al. 2020a) adds a decaying auxiliary skip connection apart from the original operations to suppress the potential advantage. iDARTS(Wang et al. 2021a) interposes a static BN layer between the node input and the operations to ensure norm consistency among different outputs. These methods make handcrafted rules and seek direct solutions, which may mistakenly reject good subnets. SNAS(Xie et al. 2018), DNAS(Hu et al. 2020) and DrNAS(Chen et al. 2020) introduce stochasticity and try different prior distributions of architecture parameters. These methods encourage exploration in the search space to boost the likelihood of parameterized candidates occurring. PC-DARTS(Xu et al. 2019) and DropNAS(Hong et al. 2022) presents dropout on feature map channels and grouped op-

erations to prevent the supernet from overfitting, but parts of the supernet may lack sufficient training.

The second type is based on the searching pipeline. DARTS+(Liang et al. 2019) and PDARTS(Chen et al. 2019) limits the number of skip connections to a constant, which is forced and suspicious. RDARTS(Zela et al. 2019) and SDARTS connects the performance collapse with the proliferation of the Hessian eigenvalues of the validation loss as an indicator. Such methods rely heavily on the quality of the indicator. SP-DARTS(Zhang and Ding 2021) and Beta-DARTS(Ye et al. 2022) adopts sparse regularized approximation and Beta-Decay regularization to adjust the distribution of the architecture parameters. PDARTS(Chen et al. 2019), SGAS(Li et al. 2020), PT(Wang et al. 2021b) and OPP-DARTS(Zhu et al. 2021) fill in the gap between the searching stage and the evaluation stage by progressively increasing the architecture depths or widths. These methods rely on emphasizing the defect of skip connections when drawing the supernet close to the selected subnet.

## 3 Methods

### 3.1 Preliminaries

In the searching stage of DARTS(Liu, Simonyan, and Yang 2018), the supernet consists of normal cells for feature extraction and reduction cells for feature downsampling. In each cell, a direct acyclic graph with  $N$  sequential nodes is connected with edges. The  $i$ -th node is an intermediate feature map  $x^{(i)}$ , and the edge  $(i, j)$  connecting the  $i$ -th node to the  $j$ -th node includes all the candidate operations  $\{o_k^{(i,j)} | k\}$  in the search space  $\mathcal{S}$ . DARTS applies continuous relaxation through trainable architecture parameters  $\alpha$  to weigh the outputs of operations. So the computation on the edge is:

$$\bar{o}^{(i,j)}(x^{(i)}) = \sum_{k=1}^{|\mathcal{S}|} \frac{\exp(\alpha_k^{(i,j)})}{\sum_{k'=1}^{|\mathcal{S}|} \exp(\alpha_{k'}^{(i,j)})} o_k^{(i,j)}(x^{(i)}) \quad (1)$$

where  $\bar{o}^{(i,j)}$  is the output of edge  $(i, j)$ . Two sets of  $\alpha = \{\alpha_k^{(i,j)} | i, j, k\}$  are respectively shared in all the normal and reduction cells. Node  $x^{(j)}$  is the summarization of all the

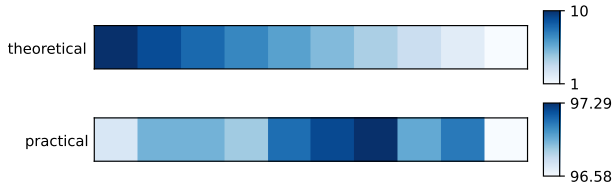


Figure 2: Experiments on operation importance represented by architecture parameters in DARTS. We always replace an operation with a less important one. The upper part shows the theoretical ranking of accuracies, while the lower part shows the practical evaluation accuracies of subnets.

edges connected with the predecessors:

$$x^{(j)} = \sum_{i < j} \bar{o}^{(i,j)}(x^{(i)}) \quad (2)$$

In this way, the discrete operation selection problem can be converted to a differentiable bi-level optimization objective:

$$\begin{aligned} \alpha^* &= \arg \min_{\alpha} \mathcal{L}_{val}(w^*(\alpha), \alpha) \\ s.t. w^*(\alpha) &= \arg \min_w \mathcal{L}_{train}(w, \alpha) \end{aligned} \quad (3)$$

Such objective assumes that the best network weights  $w^*(\alpha)$  corresponding to every set of architecture parameters  $\alpha$  can be obtained, which is unpractical due to the continuity of  $\alpha$ .

### 3.2 Rethinking the Defects in DARTS

Several methods (Chu et al. 2020a; Liang et al. 2019; Zela et al. 2019; Chen and Hsieh 2020; Chen et al. 2019) mentioned in section 2 are derived from the prior knowledge that skip connections will dominate in DARTS. They aim to alleviate the phenomenon rather than eliminate it, and therefore cannot fundamentally solve the performance collapse problem. (Chu et al. 2020a) proposes that except for a candidate operation, they also functions as an auxiliary connection to stabilize the supernet training. As a result, the architecture parameters  $\alpha$  of skip connections are unreasonably high and incommensurable with other operations. Further, an operation with a high architecture parameter merely plays an important role when all operations work together to find the correct labels. However, it is a completely different situation when the operation works alone in a subnet.  $\alpha$ 's preference to skip connections is a prominent example, considering that skip connections are of vital importance in modern CNNs (He et al. 2016). Thus, the root cause of the performance collapse is:

**Defect 1:** The architecture parameters  $\alpha$  cannot represent the importance of operations in the search space.

To demonstrate it, we conduct an experiment on DARTS that consistently replaces a more important operation represented by a higher  $\alpha$  with a less important operation represented by a lower  $\alpha$  and compares the evaluation accuracies of the two subnets. Specifically, the operations are divided into the winners and the losers in a random run of DARTS. Every time, the most important operation identified by DARTS with the highest  $\alpha$  among the winners are

replaced with the operation with the highest  $\alpha$  among the losers. Theoretically, the evaluation performance of the corresponding subnets should descend, shown in the upper part of Figure 2. However, the lower part displaying the obtained evaluation accuracies are unordered in fact. Fundamental improvements can only be achieved by exploring precise standards to represent the importance of operations.

In addition, although bi-level optimization has contributed to the success of DARTS, we find that it suffers from three crucial weaknesses:

**Defect 2:** The excessive concern over the supernet, the approximation of optimal weights and the inefficiency of data utilization in bi-level optimization can result in poor performance.

First, the losses minimized in the bi-level optimization objective are all calculated on the supernet, leading to excessive concern over the performance of the supernet. It has no relation with the validation accuracies of the subnet. We compare the final accuracies of the search and evaluation stages in several runs of DARTS in Figure 3, where the two lists of accuracies have few linear correlation. Previous researches (Chen et al. 2019; Li et al. 2020; Wang et al. 2021b,b; Zhu et al. 2021) leverage progressive pipelines to connect the two stages, but lack theoretical analysis on why such designs is superior, which is unconvincing.

Second, unlike the original objective, the actual training process optimizes the architecture parameters and network weights alternatively. The network weights are updated with only one gradient descent under fixed architecture parameters, and are served as an approximation of the optimal weights, which introduces errors and makes the results sub-optimal:

$$\begin{aligned} \nabla_{\alpha} \mathcal{L}_{val}(w^*(\alpha), \alpha) \\ \approx \nabla_{\alpha} \mathcal{L}_{val}(w - \xi \nabla_w \mathcal{L}_{train}(w, \alpha), \alpha) \end{aligned} \quad (4)$$

Third, training of both architecture parameters and network weights requires samples, which forces DARTS to divide the training set into two halves. Consequently, both trainable parameters are shown only a portion of the samples, which reduces the utilization of data and aggravates performance.

### 3.3 Precise Measurement via Fisher Information

To find the precise measurement of the importance of candidate operations, we start by assuming that after a significant and informative output feature map (FM)  $X' \in \mathbb{R}^{H \times W}$  is flattened to  $X \in \mathbb{R}^p$ , it can be estimated with a  $p$ -variate random distribution  $\mathcal{D}(\theta)$ , where  $H, W$  are the height and width of the feature map respectively,  $p = H * W$  is the total number of pixels, and  $\theta$  is the vector of  $\mathcal{D}$  parameters.

Let  $\theta(\chi)$  be an estimator that indicate how well  $\mathcal{D}(\theta)$  fits  $X$  based on the observed FMs  $\chi$ . For example, a constant function that maps to a specific  $\theta$  regardless of  $\chi$  is undoubtedly a bad estimator. Thus mean square error (MSE) is introduced to evaluate the quality of the estimator. If the optimal parameter is  $\theta^*$ , MSE is defined as:

$$L_{MSE} = \mathbb{E}[(\theta(\chi) - \theta^*)^T (\theta(\chi) - \theta^*)] \quad (5)$$

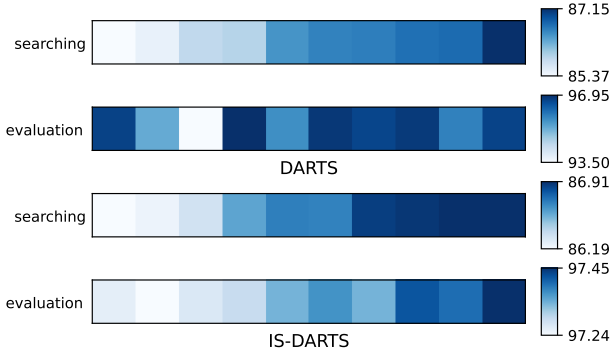


Figure 3: Comparison of the accuracies in 10 runs of DARTS and IS-DARTS. The upper part shows the searching stage while the lower shows the evaluation stage. The two color bars for DARTS have few linear correlation.

MSE can be decomposed as:

$$L_{MSE} = \text{tr}(\text{Cov}[\boldsymbol{\theta}(\chi)]) + (\mathbb{E}[\boldsymbol{\theta}(\chi)] - \boldsymbol{\theta}^*)^T (\mathbb{E}[\boldsymbol{\theta}(\chi)] - \boldsymbol{\theta}^*) \quad (6)$$

where  $\text{tr}(\cdot)$  is the trace of matrix. If the estimator is restricted to be unbiased, i.e.,  $\mathbb{E}[\boldsymbol{\theta}(\chi)] - \boldsymbol{\theta}^* = \mathbf{0}$ , MSE becomes exactly the trace of the covariance, and the estimator with the smallest values on the diagonal is the best. According to Cramer–Rao inequality, under regularity conditions, the lower bound of MSE can be calculated by:

$$\text{tr}(\text{Cov}[\boldsymbol{\theta}(\chi)]) \geq \sum_m^p \frac{1}{\mathbb{I}(\theta_m)} \quad (7)$$

where  $\mathbb{I}(\cdot)$  is the Fisher information, which is defined as:

$$\begin{aligned} \mathbb{I}(\theta_m) &= \mathbb{E} \left[ \left( \frac{\partial}{\partial \theta_m} \log f(X; \boldsymbol{\theta}) \right)^2 \right] \\ &= -\mathbb{E} \left[ \frac{\partial^2}{\partial \theta_m^2} \log f(X; \boldsymbol{\theta}) \right] \end{aligned} \quad (8)$$

where  $f(X; \boldsymbol{\theta})$  is the probability density function (PDF).

Based on the above inference, the critical distribution  $\mathcal{D}$  should be precisely determined since FMs vary with different inputs and depths in networks. However, we can in turn distinguish which FMs are insignificant by measuring whether they are close to interfering noise. Therefore, we assume that all the pixels are normally distributed and independent, i.e.,  $X \sim N_p(\boldsymbol{\mu}, \boldsymbol{\Sigma})$ , thus PDF of  $X$  can be simplified as:

$$f(X) = \frac{1}{\sqrt{2\pi}^p \prod_m^p \sigma_m} \exp \left( -\sum_m^p \frac{(x_m - \mu_m)^2}{2\sigma_m^2} \right) \quad (9)$$

where  $\boldsymbol{\Sigma} = \text{diag}(\boldsymbol{\sigma})$ . The parameters  $\boldsymbol{\theta}$  become  $\{\boldsymbol{\mu}, \boldsymbol{\sigma}\} = \{\mu_m, \sigma_m | m\}$ . According to Equation (8), the Fisher information with respect to  $\mu_m$  and  $\sigma_m$  are:

$$\begin{aligned} \mathbb{I}(\mu_m) &= \mathbb{E} \left[ \frac{1}{\sigma_m^2} \right] \\ \mathbb{I}(\sigma_m) &= \mathbb{E} \left[ \frac{3(x_m - \mu_m)^2}{\sigma_m^4} - \frac{1}{\sigma_m^2} \right] \end{aligned} \quad (10)$$

A lower bound of MSE when  $\mathcal{D}$  is  $N_p$  is obtained by substituting into the last term of Equation (7), defined as the Information-based Importance Measurement (IIM)  $\mathcal{M}$  of FMs:

$$\mathcal{M} = \sum_{\theta_m \in \boldsymbol{\mu}, \boldsymbol{\sigma}} \frac{1}{\mathbb{I}(\theta_m)} = \sum_m^p \frac{\sigma_m^2}{3} \quad (11)$$

where the variance  $\sigma_m$  is calculated across channels. When  $\mathcal{M}$  increases, the lower bound of MSE increases,  $N_p$  is a worse estimator, and  $\chi$  are less likely to be nonsensical noises. An interesting fact is that the Fisher information matrix of  $\boldsymbol{\theta}$  is a  $2p \times 2p$  matrix and has typical element:

$$(\mathbb{I}(\boldsymbol{\theta}))_{u,v} = \mathbb{E} \left[ \left( \frac{\partial}{\partial \theta_u} \log f(X; \theta_u) \right) \left( \frac{\partial}{\partial \theta_v} \log f(X; \theta_v) \right) \right] \quad (12)$$

It is easy to prove that  $\forall u \neq v, (\mathbb{I}(\boldsymbol{\theta}))_{u,v} = 0$ , thus the Fisher information matrix of  $\boldsymbol{\theta}$  is a diagonal matrix. As a result,  $\mathcal{M}$  is exactly the inverse of the sum of the Fisher information matrix. When  $\mathcal{M}$  increases, the peak around the maximum value of the log-likelihood function is shallow. Therefore from another perspective,  $\chi$  provides little information about the certainty of the parameters of the normal distribution in the estimation process and furthermore are less likely to be noises.

We can now measure the importance of operations via their output FMs, but what is the meaning of this importance for the supernet? We try to answer this question by broadening our vision from operations to nodes.

Consider the situation that the weights of the operations in the supernet are optimal after the complete training process. The intermediate FM in a node  $j$  is the sum of FMs produced by operations on edges  $\{(i, j) | i\}$ . Considering that operations are calculated separately in the forward propagation, we assume that the FM  $X_s$  in a node is the sum of  $q$  independent  $p$ -variate normal distribution, which is proved to obey a normal distribution as well according to characteristic functions:

$$X_s = \sum_n^q X_n \sim N_p(\boldsymbol{\mu}_s, \boldsymbol{\Sigma}_s) \quad (13)$$

where  $q = |\{(i, j) | i\}| * |\mathcal{S}|$  is the number of candidate operations connected to node  $j$ , and  $\boldsymbol{\mu}_s = \sum_n^q \boldsymbol{\mu}_n, \boldsymbol{\Sigma}_s = \sum_n^q \boldsymbol{\Sigma}_n$  are the sum of means and variances respectively.

According to Equation (8), the Fisher Informations with respect to the mean and the variance of the  $m$ -th element in the  $n$ -th distribution are:

$$\begin{aligned} \mathbb{I}(\mu_{ms}) &= \mathbb{E} \left[ \frac{1}{\sum_n^q \sigma_{mn}^2} \right] \\ \mathbb{I}(\sigma_{ms}) &= \mathbb{E} \left[ \frac{3(x_{ms} - \sum_n^q \mu_{mn})^2}{(\sum_n^q \sigma_{mn}^2)^2} - \frac{1}{\sum_n^q \sigma_{mn}^2} \right] \end{aligned} \quad (14)$$

where  $\sigma_{mn}$  is the  $m$ -th element of the main diagonal of  $\boldsymbol{\Sigma}_n$ . According to Equation (11), the IIM  $\mathcal{M}_s$  of the FM in the node is:

$$\mathcal{M}_s = \sum_m^p \frac{\sum_n^q \sigma_{mn}^2}{3} = \sum_n^q \mathcal{M}_n \quad (15)$$

---

**Algorithm 1: Pipeline of IS-DARTS**


---

**Input:** search space  $\mathcal{S}$ , shrink rate  $r$ 
**Output:** mask  $\Gamma$ 

- 1: initialization: mask  $\Gamma_0^* \leftarrow \mathbf{1}^{|\{(i,j)\}|*q}$ ,  $\forall h$ , reserved subset  $A_0^h \leftarrow O^h$ , discarded subset  $B_0^h \leftarrow \emptyset$
  - 2: construct supernet on  $\mathcal{S}$
  - 3: **for**  $z$  in  $[1, 1/r]$  **do**
  - 4:   **while** not converged **do**
  - 5:     train the subnet under mask  $\Gamma_{z-1}^*$  with training set
  - 6:   **end while**
  - 7:   obtain the optimal weights  $w^*(\Gamma_{z-1}^*)$
  - 8:   compute  $\mathcal{M}_z$  of operations in  $A_z$  averaged over part of validation set
  - 9:   **for all**  $h$  **do**
  - 10:     separate  $\mathcal{M}_z^h$  corresponding to  $h$ -th comparison subset
  - 11:     rank  $\mathcal{M}_z^h$  in an increasing order as  $\hat{\mathcal{M}}_z^h$
  - 12:     move  $D_z^h$  from  $A_{z-1}^h$  to  $B_{z-1}^h$  corresponding to the top  $r(|\phi^h| - C)$  values in  $\hat{\mathcal{M}}_z^h$
  - 13:     update mask  $\Gamma_{z-1}^*$  corresponding to operations in  $D_z^h$  to 0 to get  $\Gamma_z^*$
  - 14:   **end for**
  - 15: **end for**
  - 16: **return**  $\Gamma_{1/r}^*$
- 

When a constant number of operations are left in this node, they output the most significant  $X_n$ s with the maximal measurements  $\mathcal{M}_n$ s, and therefore the most significant  $X_s$ s with the maximal measurement  $\mathcal{M}_s$ . Briefly, keeping the operations with the highest IIMs in the subnet means retaining the highest IIM for the node compared to keeping the same number of other operations.

### 3.4 Improvements on Bi-level Optimization

DARTS applies the bi-level optimization due to the existence of architecture parameters  $\alpha$  and is demonstrated to suffer from crucial weaknesses in section 3.2. With IIM, we no longer rely on  $\alpha$  to select candidate operations in the training of the supernet. Instead, we adopt a binary mask  $\Gamma \in \mathbb{R}^{|\{(i,j)\}|*q}$  to represent the presence of candidates, where  $|\{(i,j)\}|$  is the number of edges in a cell. Hence the objective optimization changes to:

$$\begin{aligned} \Gamma^* &= \arg \min_{\Gamma} \mathcal{L}_{val}(w^*(\Gamma), \Gamma) \\ s.t. w^*(\Gamma) &= \arg \min_w \mathcal{L}_{train}(w, \Gamma), \forall h, \|\Gamma^h\| = C \end{aligned} \quad (16)$$

where  $\|\Gamma^h\|$  and  $C$  are determined by the requirement of the search space. In the supernet, different operations are divided into groups and compared in a winner-take-all game that selects the best  $C$  candidates. We name such a group the comparison subset  $\phi$ , then  $\cup_h \phi^h = \{o_k^{(i,j)} | i, j, k\}$ ,  $\cap^h \phi^h = \emptyset$ . For example, DARTS-based search space requires that two are selected among all the operations input to a certain node, i.e.  $\phi^h = \{o_k^{(i,h)} | i, k\}$ , so the maximum of  $h$  is the number of nodes and  $C = 2$ .  $\Gamma^h$  is the mask corresponding

to the  $h$ -th comparison subset  $\phi^h$ , therefore the concentration of the masks  $\text{concat}_h(\Gamma^h) = \Gamma$ .  $\|\Gamma^h\|$  represents the L1 norm of  $\Gamma^h$ .

Compared to Equation (3), Equation (16) is advantageous in that it focuses on the validation performance of the subnet with  $\Gamma$  covering the eliminated candidates, rather than the supernet, which is supposed to be the primary problem of DARTS.

Though  $\Gamma$  is a discrete value, both the objective function of Equation (16) that enumerate all the optimal subnets on the training set corresponding to each  $\Gamma$  and the constraint condition that evaluate all the subnets on the validation set is not computationally feasible. We simplify the proposed objective by approximating  $\mathcal{L}_{val}$ :

$$\begin{aligned} \Gamma^* &= \arg \min_{\Gamma} \Delta_{IIM}(w^*(\Gamma), \Gamma) \\ s.t. w^*(\Gamma) &= \arg \min_w \mathcal{L}_{train+val}(w, \Gamma), \forall h, \|\Gamma^h\| = C \end{aligned} \quad (17)$$

where  $\Delta_{IIM}$  is defined as the decreased IIM comparing the supernet to the subnet masked by  $\Gamma$ . Thus the selection of  $\Gamma^*$  needs no validation, and all samples can be used to train a more precise  $w^*$ .

As for the constraint condition, we further simplify Equation (17) to the one-step selection form:

$$\begin{aligned} \Gamma^* &= \arg \min_{\Gamma} \Delta_{IIM}(w^*(\Gamma), \Gamma) \\ s.t. w^*(\Gamma) &\approx w^*(\Gamma_0) = \arg \min_w \mathcal{L}_{train+val}(w, \Gamma_0), \quad (18) \\ \forall h, \|\Gamma^h\| &= C \end{aligned}$$

where  $\Gamma_0 = \mathbf{1}^{|\{(i,j)\}|*q}$  corresponds to the initial supernet. Such optimization assumes that the weights in the supernet are still optimal in the subnet under  $\Gamma$ , which obviously introduces errors.

### 3.5 Necessity of Shrinking Supernet

As mentioned above, direct one-step selection leaps from the supernet to the subnet and leads to suboptimal results. Specifically, when an operation is removed, the operations at the exact location in all the cells are removed, influencing all the intermediate FMs. In addition, the weights in the operations are no longer optimal under the contractive architecture. As a result, we need to progressively discard the operations connected to the node, followed by retraining the contractive architecture and re-measuring the importance.

We apply a greedy strategy that forces  $\|\Gamma^h\|$  to step towards  $C$  gradually. The final optimization objective is listed as:

$$\begin{aligned} \Gamma_z^* &= \arg \min_{\Gamma_z} \Delta_{IIM}(w^*(\Gamma_z), \Gamma_z) \\ s.t. w^*(\Gamma_z) &\approx w^*(\Gamma_{z-1}^*) = \arg \min_w \mathcal{L}_{train+val}(w, \Gamma_{z-1}^*), \\ \forall h, \|\Gamma_z^h\| &= C_z^h \end{aligned} \quad (19)$$

where  $z$  is the count of steps. The number of operations reserved in the comparison subset  $\phi^h$  is defined as  $C_z^h = |\phi^h| - zr(|\phi^h| - C)$ , where  $r$  is the ratio at which operations are discarded at one step. Therefore,  $C_0^h = |\phi^h|$ ,  $C_{1/r}^h = C$ ,

Table 1: Comparison with state-of-the-art methods under NAS-Bench-201 search space. The accuracies are obtained on 4 independent runs.

Method	Cost(hours)	CIFAR-10		CIFAR-100		ImageNet-6-120	
		valid	test	valid	test	valid	test
ENAS(Pham et al. 2018)	3.7	37.51±3.19	53.89±0.58	13.37±2.35	13.96±2.33	15.06±1.95	14.84±2.10
DARTS(1st)(Liu, Simonyan, and Yang 2018)	3.2	39.77±0.00	54.30±0.00	15.03±0.00	15.61±0.00	16.43±0.00	16.32±0.00
DARTS(2nd)(Liu, Simonyan, and Yang 2018)	10.2	39.77±0.00	54.30±0.00	15.03±0.00	15.61±0.00	16.43±0.00	16.32±0.00
GDAS(Dong and Yang 2019b)	8.7	89.89±0.08	93.61±0.09	71.34±0.04	70.70±0.30	41.59±1.33	41.71±0.98
SETN(Dong and Yang 2019a)	9.5	84.04±0.28	87.64±0.00	58.86±0.06	59.05±0.24	33.06±0.02	32.52±0.21
DSNAS(Hu et al. 2020)	-	89.66±0.29	93.08±0.13	30.87±16.40	31.01±16.38	40.61±0.09	41.07±0.09
PC-DARTS(Xu et al. 2019)	-	89.96±0.15	93.41±0.30	67.12±0.39	67.48±0.89	40.83±0.08	41.31±0.22
DARTS-(Chu et al. 2020a)	3.2	91.03±0.44	93.80±0.40	71.36±1.51	71.53±1.51	44.87±1.46	45.12±0.82
IS-DARTS	2.0	91.55±0.00	94.36±0.00	73.49±0.00	73.51±0.00	46.37±0.00	46.34±0.00

which connects the searching and evaluation stage. Such optimization assumes that the weights in the subnet under the mask  $\Gamma_{z-1}^*$  are still optimal in the subnet under the mask  $\Gamma_z$ , though a few operations are discarded. Condition  $\|\Gamma_z^h\| = C_z^h$  equals to finding two subsets of  $O^h$ ,  $A_z^h$  to be reserved in the subnet and  $B_z^h$  to be discarded:

$$\begin{aligned} A_z^h &= \phi^h \otimes \Gamma_z^h = \{o_{a_l^h}^h | l \in [1, C_z^h]\} \\ B_z^h &= \phi^h - \phi^h \otimes \Gamma_z^h = \{o_{b_l^h}^h | l \in [1, |\phi^h| - C_z^h]\} \end{aligned} \quad (20)$$

where  $\otimes$  means element-wise multiplication and then take out zero values,  $a_l^h, b_l^h$  are the indices of the reserved and discarded operations in  $\phi^h$  respectively.  $\forall h, z, A_z^h \cup B_z^h = \phi^h, A_z^h \cap B_z^h = \emptyset$ .

To realize the algorithm, we first train the subnet with mask  $\Gamma_{z-1}^*$  in the previous step to the optimal. Note that except for the first step that starts with a randomly initialized supernet, since  $\Gamma_z^*$  changes little compared to  $\Gamma_{z-1}^*$ , the optimal weights  $w^*(\Gamma_z^*)$  can be obtained through a few epochs of training with little error based on  $w^*(\Gamma_{z-1}^*)$ , which greatly reduces computational resources. Then The IIMs of FMs output by  $A_{z-1}^h$  is calculated as:

$$\mathcal{M}_z^h = \{\mathcal{M}_{a_l^h}^h | l \in [1, C_{z-1}^h]\} \quad (21)$$

Subsequently, the IIMs are ranked in an increasing order:

$$\begin{aligned} \hat{\mathcal{M}}_z^h &= \{\mathcal{M}_{d_l^h}^h | l \in [1, C_{z-1}^h]\} \\ s.t. \forall l_1 > l_2, \mathcal{M}_{d_{l_1}^h}^h &> \mathcal{M}_{d_{l_2}^h}^h \end{aligned} \quad (22)$$

where  $d_l^h$  is the index of the  $l$ -th highest IIM. Finally, we take the first  $r(|\phi^h| - C)$  values in  $\hat{\mathcal{M}}_z^h$  and map them to the corresponding operations:

$$D_z^h = \{o_{d_l^h}^h | l \in [1, r(|\phi^h| - C)]\} \subseteq A_{z-1}^h \quad (23)$$

$D_z^h$  is moved from  $A_{z-1}^h$  to  $B_{z-1}^h$  as  $A_z^h$  and  $B_z^h$ .

The whole algorithm is listed in Algorithm 1.

## 4 Experiments

All our experiments are implemented with Pytorch(Paszke et al. 2017) and conducted on NVIDIA GTX 3090 GPUs.

Table 2: Comparison with state-of-the-art methods under DARTS search space on CIFAR-10. The accuracies are obtained on 4 independent runs.

Architecture	Test Error (%)	Params (M)	Cost (GPU Days)	Search Method
DenseNet-BC(Huang et al. 2017)	3.46	25.6	-	manual
NASNet-A(Zoph et al. 2018)	2.65	3.3	2000	RL
AmoebaNet-A(Real et al. 2019)	3.34±0.06	3.2	3150	EA
AmoebaNet-B(Real et al. 2019)	2.55±0.05	2.8	3150	EA
Hierarchical-EAS(Liu et al. 2017)	3.75±0.12	15.7	300	EA
PNAS(Liu et al. 2018)	3.41±0.09	3.2	225	SMBO
ENAS(Pham et al. 2018)	2.89	4.6	0.5	RL
DARTS(1st)(Liu, Simonyan, and Yang 2018)	3.00±0.14	3.3	1.5	gradient
DARTS(2nd)(Liu, Simonyan, and Yang 2018)	2.76±0.09	3.3	4	gradient
SNAS(Xie et al. 2018)	2.85±0.02	2.8	1.5	gradient
GDAS(Dong and Yang 2019b)	2.82	2.5	0.17	gradient
SGAS(Li et al. 2020)	2.67±0.21	3.9	0.25	gradient
P-DARTS(Chen et al. 2019)	2.50	3.4	0.3	gradient
PC-DARTS(Xu et al. 2019)	2.57±0.07	3.6	0.1	gradient
FairDARTS(Chu et al. 2020b)	2.54±0.05	3.32±0.46	-	gradient
SDARTS-ADV(Chen and Hsieh 2020)	2.61±0.02	3.3	1.3	gradient
DARTS-(Chu et al. 2020a)	2.59±0.08	3.5±0.13	0.4	gradient
IS-DARTS	2.56±0.04	4.25±0.22	0.42	gradient

### 4.1 Results on NAS-Bench-201 Search Space

**Settings.** As the most widely used NAS benchmark, NAS-Bench-201(Dong and Yang 2020) provides the performance of 15,625 architectures on three datasets(CIFAR-10, CIFAR-100 and ImageNet). The comparison subset in NAS-Bench-201 is operations on a certain edge and  $C = 1$ . We keep the searching and evaluation settings same as those of DARTS in (Dong and Yang 2020), except that the searching epoch is decreased to 30 in order to reduce consumption. Specific architectures and hyper-parameters are shown in Appendix A.1. The shrink rate  $r$  in IS-DARTS is 0.25, and the epoch interval between steps is 2. 200 samples of the validation set are used to calculate a precise and stable IIM, which will be proved in section 4.3.

**Results.** The mean and standard deviation of 4 independent runs with different random seeds of IS-DARTS is presented in Table 1. The architecture found on CIFAR-10 achieves consistent state-of-the-art performance on all the three datasets, showing the superiority and generalization of IS-DARTS. It significantly outperforms DARTS by 113.43% on average by tackling the performance collapse problem. In addition, since IS-DARTS only searches on CIFAR-10 with fewer epochs and requires few extra computational resources, it reduces the searching cost by 37.5% compared to DARTS.

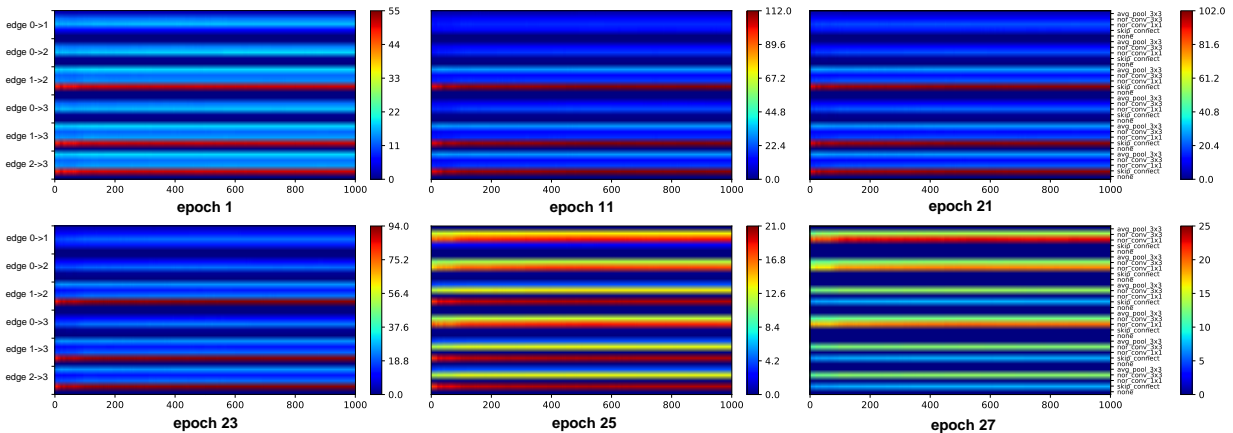


Figure 4: The IIMs of operations on all edges at different epochs in the searching stage. The x-axis represents the number of input images, and the y-axis represents operations at different locations in the cell. The mapping relation between colors and IIMs is shown in the right bars.

## 4.2 Results on DARTS Search Space

**Settings.** Classical DARTS search space(Liu, Simonyan, and Yang 2018) is another important benchmark for evaluating NAS methods. In the searching stage, the architecture is selected under CIFAR-10 dataset. The comparison subset in the DARTS search space is all the operations input into a certain node and  $C = 2$ . Then in the evaluation stage, the architecture is evaluated on CIFAR-10 and transferred to ImageNet. All the searching and evaluation settings are kept the same as those of DARTS(Liu, Simonyan, and Yang 2018) in Appendix A.2 . The shrink rate in IS-DARTS is 0.143 and the epoch interval between steps is 3. 600 samples of the validation set are used to calculate the IIM.

**Results.** Table 2 summarizes the performance of IS-DARTS on CIFAR-10 compared to handcrafted architectures and NAS methods. With extremely low computational costs in the searching stage, the average test accuracy of 4 independent runs is  $97.44 \pm 0.04\%$ , basically same as state-of-the-art methods. To verify the generalization ability, architecture found on CIFAR-10 can still ensure a state-of-the-art performance, namely 75.9% on ImageNet. IS-DARTS surpasses all the methods that search on CIFAR-10, and is comparable to the methods that search directly on ImageNet and take more than  $7 \times$  GPU days. The impressive results demonstrate the effectiveness and efficiency of IS-DARTS.

## 4.3 Stability

To further understand the mechanism of IS-DARTS, we visualize the IIMs in the searching process under NAS-Bench-201 as the number of the input images randomly sampled from CIFAR-10 increase from 1 to 1000 in Figure 4. In the beginning of the searching stage, the steady rise of the information means the network is learning. However, the decline appears at around epoch 20, which would be explained by overfitting. It is evident that skip connections are crucial in the training of the supernet, far beyond other operations at epoch 11. After two shrinking steps, i.e. epoch 25 and 27, several operations in the search space are discarded, and

Table 3: Comparison with state-of-the-art methods under DARTS search space on ImageNet. The dataset on which the architecture is searched is shown behind the methods. I represents ImageNet and C represents CIFAR-10.

Architecture	Test Error(%)		Params (M)	Cost (GPU Days)	Search Method
	top-1	top-5			
Inception-v1(Szegedy et al. 2015)	30.2	10.1	6.6	-	manual
MobileNet(Howard et al. 2017)	29.4	10.5	4.2	-	manual
ShuffleNet 2x(Zhang et al. 2018)	26.3	-	$\sim 5$	-	manual
NASNet-A(Zoph et al. 2018)	26	8.4	5.3	2000	RL
NASNet-B(Zoph et al. 2018)	27.2	8.7	5.3	2000	RL
NASNet-C(Zoph et al. 2018)	27.5	9	4.9	2000	RL
AmoebaNet-A(Real et al. 2019)	25.5	8	5.1	3150	EA
AmoebaNet-B(Real et al. 2019)	26	8.5	5.3	3150	EA
AmoebaNet-C(Real et al. 2019)	24.3	7.6	6.4	3150	EA
PNAS(Liu et al. 2018)	25.8	8.1	5.1	$\sim 225$	SMBO
DARTS(Liu, Simonyan, and Yang 2018)(C)	26.7	8.7	4.7	4	gradient
SNAS(Xie et al. 2018)(C)	27.3	9.2	4.3	1.5	gradient
GDAS(Dong and Yang 2019b)(C)	27.5	9.1	4.4	0.17	gradient
SGAS(Li et al. 2020)(C)	24.38	7.39	5.4	0.25	gradient
P-DARTS(Chen et al. 2019)(C)	24.4	7.4	4.9	0.3	gradient
PC-DARTS(Xu et al. 2019)(I)	24.2	7.3	5.3	3.8	gradient
FairDARTS(Chu et al. 2020b)(I)	24.4	7.4	4.3	3	gradient
SDARTS-ADV(Chen and Hsieh 2020)(C)	25.2	7.8	-	-	gradient
DARTS-(Chu et al. 2020a)(I)	23.8	7	4.9	4.5	gradient
IS-DARTS(C)	24.1	7.1	6.4	0.42	gradient

therefore the information of the skip connections decreases sharply without their assistance. Convolutional operations start to show their strengths and finally contribute to the excellent performance of the selected subnet in IS-DARTS. In addition, the IIM metric shows its efficiency that it stabilizes with conservatively 200 inputs and costs few extra resources.

## 5 Conclusion

In this paper, we propose Information-based Shrinking DARTS(IS-DARTS). We precisely measure the importance of candidate operations in the search space via Fisher information metric, and reformulate the bi-level optimization problem into a more accurate and efficient form focusing on the performance of subnets. Furthermore, we adopt a shrinking pipeline on the comparison subsets of the supernet. The remarkable performance of IS-DARTS demonstrates its ability to search for stable and outstanding neural architectures and apply in practical deep learning problems.

## 6 Acknowledgments

This work was supported by the National Basic Strengthen Research Program of ReRAM under Grant2022-00-03, Natural Science Foundation of ShaanxiProvince, China under Grant 2022JM-366 and by the Open-End Fund of Beijing Institute of Control Engineering under Grant OBCandETL-2022-03.

## References

- Baker, B.; Gupta, O.; Naik, N.; and Raskar, R. 2016. Designing neural network architectures using reinforcement learning. *arXiv preprint arXiv:1611.02167*.
- Chen, X.; and Hsieh, C.-J. 2020. Stabilizing differentiable architecture search via perturbation-based regularization. In *International conference on machine learning*, 1554–1565. PMLR.
- Chen, X.; Wang, R.; Cheng, M.; Tang, X.; and Hsieh, C.-J. 2020. Dnns: Dirichlet neural architecture search. *arXiv preprint arXiv:2006.10355*.
- Chen, X.; Xie, L.; Wu, J.; and Tian, Q. 2019. Progressive differentiable architecture search: Bridging the depth gap between search and evaluation. In *Proceedings of the IEEE/CVF international conference on computer vision*, 1294–1303.
- Chu, X.; Wang, X.; Zhang, B.; Lu, S.; Wei, X.; and Yan, J. 2020a. Darts-: robustly stepping out of performance collapse without indicators. *arXiv preprint arXiv:2009.01027*.
- Chu, X.; Zhou, T.; Zhang, B.; and Li, J. 2020b. Fair darts: Eliminating unfair advantages in differentiable architecture search. In *Computer Vision—ECCV 2020: 16th European Conference, Glasgow, UK, August 23–28, 2020, Proceedings, Part XV*, 465–480. Springer.
- Dong, X.; and Yang, Y. 2019a. One-shot neural architecture search via self-evaluated template network. In *Proceedings of the IEEE/CVF International Conference on Computer Vision*, 3681–3690.
- Dong, X.; and Yang, Y. 2019b. Searching for a robust neural architecture in four gpu hours. In *Proceedings of the IEEE/CVF Conference on Computer Vision and Pattern Recognition*, 1761–1770.
- Dong, X.; and Yang, Y. 2020. Nas-bench-201: Extending the scope of reproducible neural architecture search. *arXiv preprint arXiv:2001.00326*.
- He, K.; Zhang, X.; Ren, S.; and Sun, J. 2016. Deep residual learning for image recognition. In *Proceedings of the IEEE conference on computer vision and pattern recognition*, 770–778.
- Hong, W.; Li, G.; Zhang, W.; Tang, R.; Wang, Y.; Li, Z.; and Yu, Y. 2022. Dropnas: Grouped operation dropout for differentiable architecture search. *arXiv preprint arXiv:2201.11679*.
- Howard, A. G.; Zhu, M.; Chen, B.; Kalenichenko, D.; Wang, W.; Weyand, T.; Andreetto, M.; and Adam, H. 2017. Mobilenets: Efficient convolutional neural networks for mobile vision applications. *arXiv preprint arXiv:1704.04861*.
- Hu, S.; Xie, S.; Zheng, H.; Liu, C.; Shi, J.; Liu, X.; and Lin, D. 2020. Dsnas: Direct neural architecture search without parameter retraining. 2020 IEEE. In *CVF Conference on Computer Vision and Pattern Recognition (CVPR)*, 12081–12089.
- Huang, G.; Liu, Z.; Van Der Maaten, L.; and Weinberger, K. Q. 2017. Densely connected convolutional networks. In *Proceedings of the IEEE conference on computer vision and pattern recognition*, 4700–4708.
- Li, G.; Qian, G.; Delgadillo, I. C.; Muller, M.; Thabet, A.; and Ghanem, B. 2020. Sgas: Sequential greedy architecture search. In *Proceedings of the IEEE/CVF Conference on Computer Vision and Pattern Recognition*, 1620–1630.
- Liang, H.; Zhang, S.; Sun, J.; He, X.; Huang, W.; Zhuang, K.; and Li, Z. 2019. Darts+: Improved differentiable architecture search with early stopping. *arXiv preprint arXiv:1909.06035*.
- Liu, C.; Zoph, B.; Neumann, M.; Shlens, J.; Hua, W.; Li, L.-J.; Fei-Fei, L.; Yuille, A.; Huang, J.; and Murphy, K. 2018. Progressive neural architecture search. In *Proceedings of the European conference on computer vision (ECCV)*, 19–34.
- Liu, H.; Simonyan, K.; Vinyals, O.; Fernando, C.; and Kavukcuoglu, K. 2017. Hierarchical representations for efficient architecture search. *arXiv preprint arXiv:1711.00436*.
- Liu, H.; Simonyan, K.; and Yang, Y. 2018. Darts: Differentiable architecture search. *arXiv preprint arXiv:1806.09055*.
- Long, J.; Shelhamer, E.; and Darrell, T. 2015. Fully convolutional networks for semantic segmentation. In *Proceedings of the IEEE conference on computer vision and pattern recognition*, 3431–3440.
- Paszke, A.; Gross, S.; Chintala, S.; Chanan, G.; Yang, E.; DeVito, Z.; Lin, Z.; Desmaison, A.; Antiga, L.; and Lerer, A. 2017. Automatic differentiation in pytorch.
- Pham, H.; Guan, M.; Zoph, B.; Le, Q.; and Dean, J. 2018. Efficient neural architecture search via parameters sharing. In *International conference on machine learning*, 4095–4104. PMLR.
- Real, E.; Aggarwal, A.; Huang, Y.; and Le, Q. V. 2019. Regularized evolution for image classifier architecture search. In *Proceedings of the aaai conference on artificial intelligence*, volume 33, 4780–4789.
- Real, E.; Moore, S.; Selle, A.; Saxena, S.; Suematsu, Y. L.; Tan, J.; Le, Q. V.; and Kurakin, A. 2017. Large-scale evolution of image classifiers. In *International Conference on Machine Learning*, 2902–2911. PMLR.
- Ren, S.; He, K.; Girshick, R.; and Sun, J. 2015. Faster r-cnn: Towards real-time object detection with region proposal networks. *Advances in neural information processing systems*, 28.
- Szegedy, C.; Liu, W.; Jia, Y.; Sermanet, P.; Reed, S.; Anguelov, D.; Erhan, D.; Vanhoucke, V.; and Rabinovich, A. 2015. Going deeper with convolutions. In *Proceedings of the IEEE conference on computer vision and pattern recognition*, 1–9.
- Wang, H.; Yang, R.; Huang, D.; and Wang, Y. 2021a. idarts: Improving darts by node normalization and decorrelation



discretization. *IEEE Transactions on Neural Networks and Learning Systems*.

Wang, R.; Cheng, M.; Chen, X.; Tang, X.; and Hsieh, C.-J. 2021b. Rethinking architecture selection in differentiable nas. *arXiv preprint arXiv:2108.04392*.

Xie, S.; Zheng, H.; Liu, C.; and Lin, L. 2018. SNAS: stochastic neural architecture search. *arXiv preprint arXiv:1812.09926*.

Xu, Y.; Xie, L.; Zhang, X.; Chen, X.; Qi, G.-J.; Tian, Q.; and Xiong, H. 2019. Pc-darts: Partial channel connections for memory-efficient architecture search. *arXiv preprint arXiv:1907.05737*.

Ye, P.; Li, B.; Li, Y.; Chen, T.; Fan, J.; and Ouyang, W. 2022.  $\beta$ -DARTS: Beta-Decay Regularization for Differentiable Architecture Search. In *2022 IEEE/CVF Conference on Computer Vision and Pattern Recognition (CVPR)*, 10864–10873. IEEE.

Zela, A.; Elsken, T.; Saikia, T.; Marrakchi, Y.; Brox, T.; and Hutter, F. 2019. Understanding and robustifying differentiable architecture search. *arXiv preprint arXiv:1909.09656*.

Zhang, J.; and Ding, Z. 2021. Robustifying DARTS by Eliminating Information Bypass Leakage via Explicit Sparse Regularization. In *2021 IEEE International Conference on Data Mining (ICDM)*, 877–885. IEEE.

Zhang, X.; Zhou, X.; Lin, M.; and Sun, J. 2018. Shufflenet: An extremely efficient convolutional neural network for mobile devices. In *Proceedings of the IEEE conference on computer vision and pattern recognition*, 6848–6856.

Zhu, X.; Li, J.; Liu, Y.; Liao, J.; and Wang, W. 2021. Operation-level Progressive Differentiable Architecture Search. In *2021 IEEE International Conference on Data Mining (ICDM)*, 1559–1564. IEEE.

Zoph, B.; Vasudevan, V.; Shlens, J.; and Le, Q. V. 2018. Learning transferable architectures for scalable image recognition. In *Proceedings of the IEEE conference on computer vision and pattern recognition*, 8697–8710.

# Supplementary Material

## A Training Settings

### A.1 NAS-Bench-201 search space

The supernet is stacked by  $N = 5$  cells in each of the 3 blocks and each cell is constructed by  $V = 4$  nodes connected with  $E = 6$  edges. Each edge contains all the operations in the search space  $\mathcal{S}$ : zero, skip connection,  $1 \times 1$  convolution,  $3 \times 3$  convolution, and  $3 \times 3$  average pooling.

The random horizontal flipping, random cropping with padding, and normalization are used for data augmentation. We train the supernet with Nesterov momentum SGD for 30 epochs. The weight decay is 0.0005 and the momentum is 0.9. We decay the learning rate from 0.025 to 0.001 with cosine scheduler and clip the gradient by 5. The batch size is set to 64.

### A.2 DARTS-based search space

The supernet consists of 8 cells, where the third and sixth cells are the reduction cells that connects  $N = 2$  normal cells in each block. Each cell has 2 inputs (the outputs of the previous cell and the cell before the previous cell) and  $V = 4$  intermediate nodes connected with  $E = 14$  edges. The search space contains zero, skip connection,  $3 \times 3$  and  $5 \times 5$  separable convolutions,  $3 \times 3$  and  $5 \times 5$  dilated separable convolutions,  $3 \times 3$  max pooling and  $3 \times 3$  average pooling.

In the searching stage, the supernet is trained on CIFAR-10 with Nesterov momentum SGD for 50 epochs. The other hyper-parameters and the data augmentation methods remain the same as in section A.1. The architecture is shown in Figure A.2.

In the evaluation on CIFAR-10, a deeper subnet with  $N = 3$  is trained for totally 600 epochs with a warmup of 5 epochs. The batch size is 96. The other hyper-parameters remain the same as those used for searching. Moreover, we use additional enhancements including cutout, path dropout of probability 0.2 and auxiliary towers with weight 0.4.

In the evaluation on ImageNet,  $N$  changes to 4. Data augmentation include random cropping, color jittering, lighting, random horizontal flipping and normalization. The subnet is trained for 250 epochs with a warmup of 5 epochs, a batch size of 128, a momentum of 0.9 and a weight decay of 0.00003. The learning rate decay from 0.1 to 0 following a cosine scheduler.

## B Ablation Study

We explore the influence of removing the selection via IIMs and the shrinking pipeline, denoted as S-DARTS and I-DARTS respectively. The ablation is done on NAS-Bench-201 search space, and the parameters of S-DARTS keeps the same as IS-DARTS. The results is shown in Table A.1.

S-DARTS fails to resolve the fundamental problem of performance collapse with only the shrinking pipeline and ends up with the architecture shown in Figure A.1(a), dominated by parameter-free operations. The final architecture of I-DARTS is Figure A.1(b), which shows some improvements in the middle of the cells. Wrong decision occurs on all the edges connected to the input of the cells, in that the skip

Table A.1: Ablation Study on the pipelines under NAS-Bench-201.

Method	CIFAR-10		CIFAR-100		ImageNet-6-120	
	valid	test	valid	test	valid	test
IS-DARTS	91.55	94.36	73.49	73.51	46.37	46.34
I-DARTS	90.59	93.31	70.05	69.83	43.78	43.84
S-DARTS	68.29	70.92	38.57	38.97	18.87	18.41

connections which directly bypass all the information extracted by the previous cell is naturally superior to the other operations. In contrast, the shrinking pipeline of IS-DARTS weakens the role of skip connections and makes them comparable with the other operations by steps.

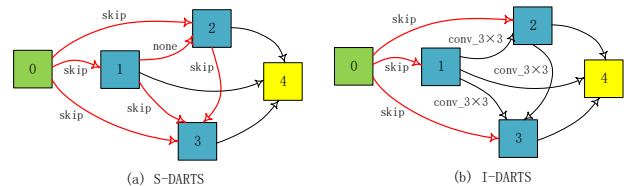


Figure A.1: Architecture found by I-DARTS and S-DARTS under NAS-Bench-201 search space.

We also conduct ablation studies on different shrink rates under DARTS search space. We adjust the interval epoch to ensure that shrinking only happens in the last 20 epochs. The results are shown in Table A.2. When the shrink rate fluctuates within a reasonable range, the evaluation performance is basically consistent. When the shrink rate is close to 0, the supernet lacks sufficient training in less interval epochs. When the shrink rate is close to 1, the gap of supernet in adjacent steps becomes larger. Both situations worsen the performance. Specially, when the shrink rate is 1, IS-DARTS degrades to I-DARTS.

Table A.2: Ablation Study on different shrink rates under DARTS search space.

shrink rate	1 (I-DARTS)	0.5	0.25	0.143	0.1	0.05
interval epoch	/	18	6	3	2	1
test error	2.98	2.87	2.51	2.56	2.58	2.95

## C Extra Visualization

We conduct IS-DARTS on NAS-Bench-201 benchmark and CIFAR-100 dataset and achieve 70.71% validation accuracy and 71.11% test accuracy. We visualize the IIMs during searching in the same way as Figure 4. Figure A.3 illustrates that IS-DARTS stabilizes with approximately 500 samples.

Following Fig. 3 in FairDarts, we visualize the softmax of the architecture parameters in DARTS and the smoothed softmax of information measurements in IS-DARTS in Figure A.4. It is clearly demonstrated that the IIMs of parameter-free candidates drop sharply once a parameterized candidate is discarded, and performance collapse is resolved in consequence.

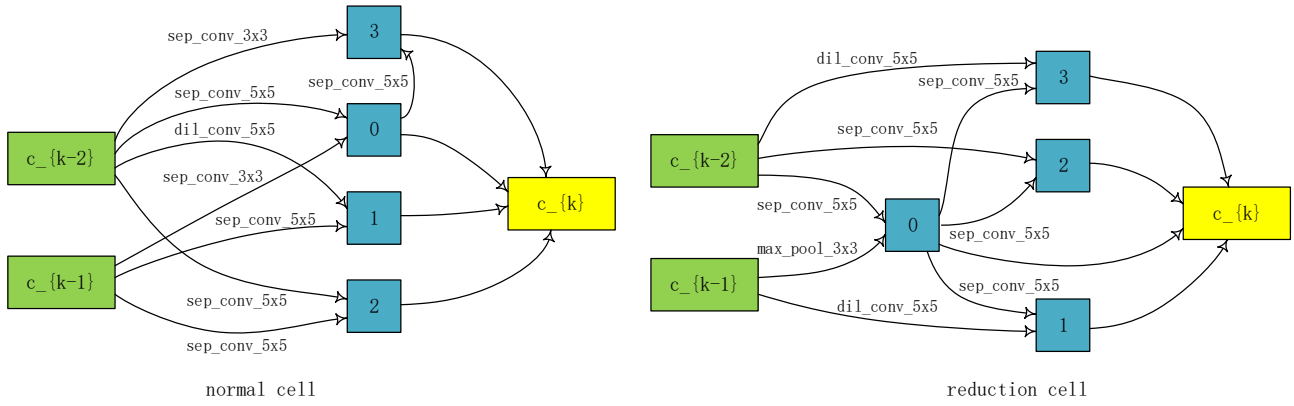


Figure A.2: Normal cell and reduction cell found by IS-DARTS on CIFAR-10 under DARTS search space.

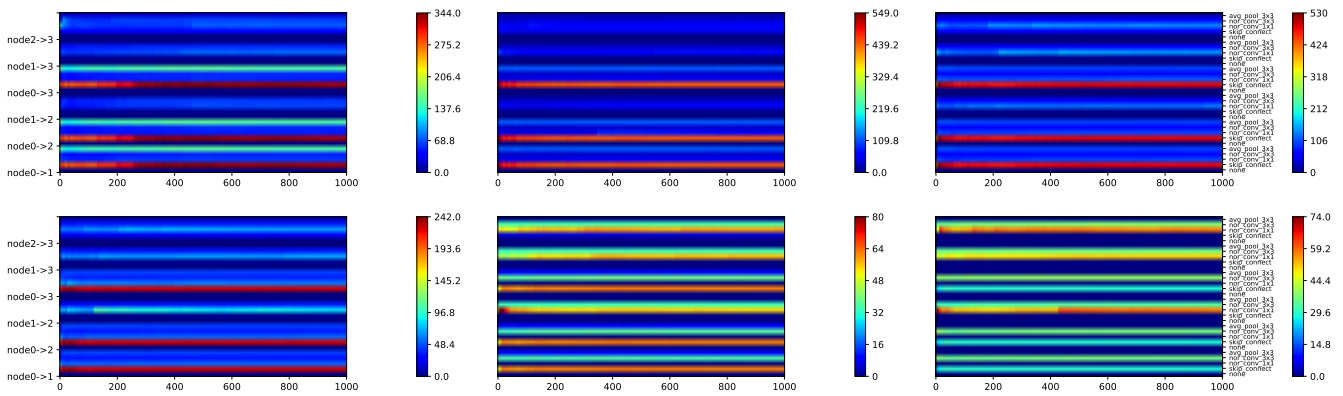


Figure A.3: The IIMs of operations on all edges at different epochs in the searching stage on NAS-Bench-201 and CIFAR-100.

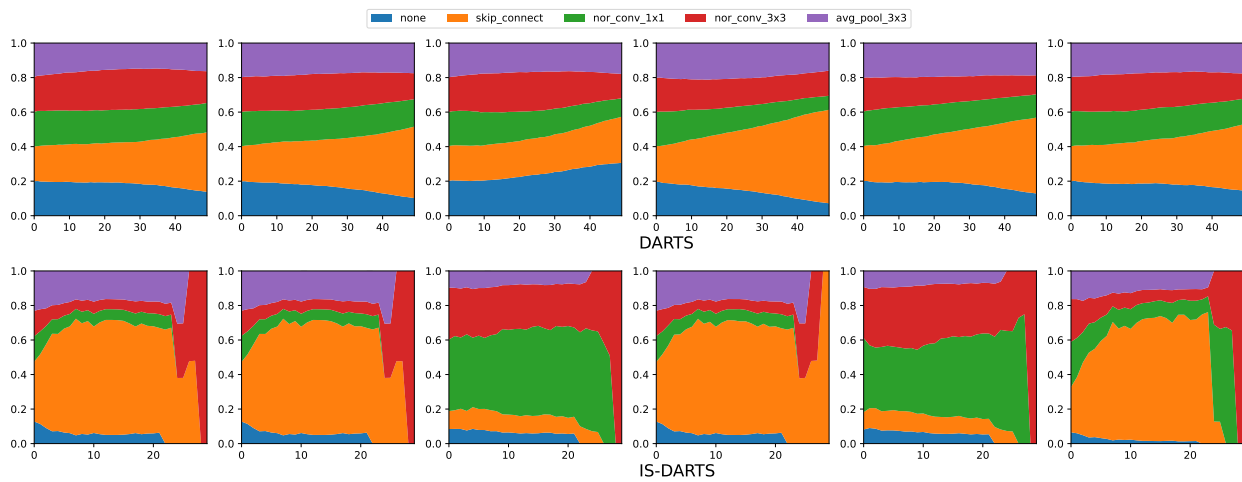


Figure A.4: The softmax of the architecture parameters in DARTS and the smoothed softmax of information measurements in IS-DARTS under NAS-Bench-201.